THE ASTROPHYSICAL JOURNAL, 394:51–60, 1992 July 20

GRAVITATIONAL LENSING OF QUASARS AS SEEN BY THE *HUBBLE SPACE TELESCOPE* SNAPSHOT SURVEY[1]

D. MAOZ,[2,3] J. N. BAHCALL,[2] R. DOXSEY,[4] D. P. SCHNEIDER,[2,3] N. A. BAHCALL,[5]
O. LAHAV,[6] AND B. YANNY[2,7]

Received 1991 December 11; accepted 1992 January 28

ABSTRACT

As part of the ongoing *HST* Snapshot Survey, 152 additional high-luminosity $z > 1$ quasars were observed, bringing the total to 184 quasars. Each exposure was searched for evidence of gravitational lensing. Only one quasar among those observed, 1208+1011, is a candidate lens system with subarcsecond image separation. Six other quasars have point sources within 6″. Ground-based observations of five of these cases show that the companion point sources are foreground Galactic stars. The observed lensing frequency, after accounting for known lenses excluded from the sample, and including 32 quasars observed from a pilot sample described in a previous paper, is 3/184. The predicted lensing frequency of the sample is calculated for a variety of cosmological models. The effect of uncertainties in some of the observational parameters upon the predictions is discussed. The observed lensing frequency is consistent with predictions of models with a zero cosmological constant λ. Assuming the best estimates for the parameters involved in the calculation, flat cosmologies with $\lambda > 0.85$ can be ruled out at greater than 95% confidence. From the engineering perspective, we find that the software corrections for stellar aberration when the telescope is guided on gyroscopes results in drift rates of 1–2 milliarcseconds s^{-1}, about 3 times smaller than before the correction was implemented. The mean and rms pointing error under gyro control is $20'' \pm 13''$. We find no correlation of the drift rate with time, right ascension, declination, or pointing error.

Subject headings: gravitational lensing — quasars: general — surveys

1. INTRODUCTION

The phenomenon of gravitational lensing allows new insight into many fundamental astrophysical problems: The dark matter problem (Tyson, Valdes, & Wenk 1990; Paczyński 1986), the value of H_0 (Chang & Refsdal 1979), the existence of a cosmological constant (Fukugita & Turner 1991), the sizes of quasar continuum emission regions (Rauch & Blandford 1991), and tests of general relativity (Dar 1992), to name a few (see Blandford & Narayan 1992 for a review). During the past 13 years, 10 cases of probable lensing of quasars have been found (e.g., Kochanek 1991a). All of these lenses have image separations greater than $\sim 1''$. Theoretical models (e.g., Turner, Ostriker, & Gott 1984; Kochanek 1991b; Fukugita & Turner 1991) predict, however, that about one-half of all gravitationally lensed quasars have subarcescond image separations and are therefore difficult to identify with ground-based observations.

The Snapshot Survey is a search for cases of gravitational lensing among 354 intrinsically luminous, high-redshift quasars using the *Hubble Space Telescope* (*HST*) Planetary Camera (PC). Despite the spherical aberration of *HST*'s primary mirror, the sharp core of the point-spread function affords the high spatial resolution needed to discover the small-separation lenses. The Snapshot Survey is also sensitive to large image-separation lenses, and is one of few studies in which a large, well-defined quasar sample is systematically searched for lensing. A previous paper (Bahcall et al. 1992, hereafter Paper I) described in detail the objectives of the survey, its mode of operation, and the sample definition. We will summarize here only the main points. The discovery of a possible subarcsecond lens system, 1208+1011, is reported in Maoz et al. (1992).

The Snapshot Survey involves short exposures (260 s) taken during gaps in the scheduled observing program, when the telescope would otherwise be idle. Snapshot targets are assigned only after all other programs have been scheduled. Most images are obtained using only the gyroscopes for pointing and guiding, thus saving the time necessary to acquire guide stars. Targets are distributed throughout the sky, so only short slews (typically a few degrees) are required to move the telescope from any approved science target to a nearby Snapshot target. The data are nonproprietary, and can be obtained from the Space Telescope Science Institute's (STScI) Data Systems Operations Branch.

The sample consists of all quasars in the catalog of Véron-Cetty & Véron (1987) with a redshift greater than 1, an absolute magnitude M_V brighter than -25.5, and Galactic latitude $|b| > 10°$. Absolute magnitudes were calculated using a Hubble constant of $H_0 = 100$ km s^{-1} Mpc^{-1}, deceleration parameter $q_0 = 0.5$, k-corrections assuming an optical power-law spectral index of -0.5, and Galactic absorption corrections from de Vaucouleurs, de Vaucouleurs, & Corwin (1976). Excluded from the sample were quasars having very bright stars nearby in the field of view and quasars that were to be observed as part of other *HST* imaging programs (see Paper I).

[1] Based on observations with the NASA/ESA *Hubble Space Telescope*, obtained at the Space Telescope Science Institute, which is operated by the Association of Universities for Research in Astronomy, Inc., under NASA contract NAS5-26555.

[2] Institute for Advanced Study, Princeton, NJ 08540.
[3] Guest Investigator, Palomar Observatory, California Institute of Technology.
[4] Space Telescope Science Institute, 3700 San Martin Drive, Baltimore, MD 21218.
[5] Princeton University Observatory, Princeton, NJ 08544.
[6] Institute of Astronomy, Madingley Road, Cambridge CB3 0HA, England.
[7] Apache Point Observatory, Astrophysical Research Consortium.

Paper I reported observations of a pilot sample which was used to determine the feasibility of the program and its optimal mode of operation. About 30 quasars were successfully observed, none of which showed multiple components indicative of gravitational lensing. Paper I also uncovered and led to the correction of several software errors in the *HST* ground support system. Most important, we found that the lack of correction for stellar aberration when the telescope was guided solely on gyroscopes caused large telescope drift rates (≈ 4.5 milliarcseconds s^{-1}), and large pointing errors which caused approximately one-half of the target quasars to be outside the PC field of view.

In the present paper we report the results of the Snapshot Survey following observations of about one-half of the entire quasar sample. Section 2 describes the observations. The analysis and results for some notable objects are presented in § 3. Section 4 gives the engineering information acquired from these data. In § 5 we calculate the lensing frequency predicted by a variety of theoretical models, compare it with our observations, and discuss the implications. Section 6 summarizes our main conclusions.

2. OBSERVATIONS

This paper describes the Snapshot Survey observations carried out between 1991 April 14 and 1991 September 22 under *HST* programs 3156–3159. Together with the observations in Paper I, about one-half of our sample of 354 quasars was observed during this period. Observations of the rest of the sample will be described in a future paper.

Each quasar was observed for 260 s with the F555W filter. Note that this differs from the observations of the pilot sample in Paper I, where each quasar was observed in both F555W and F785LP and the exposure length was either 2 or 4 minutes. The observation in only one bandpass in the current program is intended to maximize the number of objects actually observed. F555W (similar to the Johnson *V* band) was chosen, since it is one of the more efficient bands (see also § 4); the efficiency in F785LP may be a factor of 2 lower than prelaunch expectations (Horne & Ritchie 1991).

The designated target location on the PC was on the PC-6 CCD chip, 10″ in the column and row directions away from the center of the CCD mosaic. At STScI's direction, some of the exposures were carried out using Fine Guidance Sensor "coarse track" guiding, rather than the usual gyroscope guiding.

The observations described in this paper are summarized in Table 1. The first column gives the quasar name, excluding any prefixes to the 1950 coordinates. The second column gives another name for the object in cases where Véron-Cetty & Véron (1987) list the object under that name. The third column gives the UT date on which the object was observed by *HST* (day/month/year), and the fourth column gives the *HST* program number (the sample was arbitrarily divided into four separate programs, according to right ascension). The fifth column gives the PC CCD chip (5–8) on which the quasar actually appears, and the quasar's central pixel coordinates, where the pixel of each CCD that is nearest to the center of the mosaic has coordinates (1, 1). A "missed" entry in this column indicates that the quasar was nowhere in the PC field of view (15 such cases). Column (6) gives the offset in arcseconds from the designated position. Column (7) gives the drift rate in milliarcseconds (mas) s^{-1} as measured from the length of the trail of the quasar or a star in the field of view. Exposures that were coarse track–guided (i.e., untrailed) are marked by a "g" in this column (36 such cases). Column (8) gives the *V*-magnitude measured for each object observed. This was calculated by summing the counts inside a 60 pixel (2.″6) radius, subtracting the median sky value determined in an 80–100 pixel annulus, and assuming that one electron corresponds to $V = 31.4$ (Griffiths 1990). No attempt was made to remove cosmic-ray events. Columns (9) and (10) give the *V*-magnitude and the redshift tabulated by Véron-Cetty & Véron (1987), while column (11) gives the absolute magnitude, calculated as described in § 1. Column (12) gives coded comments, which are generally of a technical nature, for some of the objects. Objects for which the comments are of a more scientific nature are coded with an "A" and are further described in § 3.2, "Notes on Individual Objects."

Of the 168 exposures, only 15 missed the target. This compares with the $\approx 50\%$ failure rate in the pilot study described in Paper I (see § 4 for further discussion of the telescope pointing). As indicated in the "Comments" column of Table 1, in only one of the remaining 153 exposures is there reasonable doubt concerning the identification of the quasar in the field of view. Two of the quasars observed here were also observed in Paper I, where one was missed (0201+36B) and the identification of another (0451−418) was uncertain. Both quasars are verified to be in the field of view this time.

As in Paper I, we have carried out supporting ground-based observations for some of the Snapshot exposures. These were carried out at the Palomar 5 m telescope with the 4-Shooter spectrograph (Gunn et al. 1987), the Palomar 1.5 m telescope with an 800 × 800 Texas Instruments CCD, the Cerro-Tololo Inter-American Observatory (CTIO) 0.9 m telescope with a Tektroniks 512 × 512 CCD, and the Astrophysical Research Consortium (ARC) Apache Point 1.8 m telescope with an 800 × 800 Texas Instruments CCD. These observations are described in "Notes on Individual Objects" in § 3.2. Supporting ground-based observations for several objects from Paper I are described in § 3.3, "Notes on Objects from Paper I."

3. ANALYSIS

3.1. *Detection Limits*

As in Paper I, each *HST* exposure was examined by eye for evidence of gravitational lensing. In Paper I, the limits for detection of multiple images were estimated by simulations designed to reproduce the conditions of the actual exposures. The simulations used a trailed point-spread function that was 0.″55 long (corresponding to a trail rate of 2.1 mas s^{-1} in the present 260 s exposures), a primary image with a total of 120,000 electrons (corresponding to a $V = 18.7$ mag object in a 260 s exposure), and secondary components of various magnitudes. As seen in Table 1, these values for the trail rate and the primary component magnitude are representative of many of our exposures but are more typical of the fainter objects and the longer trails. In Paper I, we found that the detection limits have no strong dependence on the brightness of the primary image, but rather depend mainly on the magnitude differences between the primary and the secondary. As we will show below, the detection capabilities are slightly improved when the trails are shorter. The detection limits found in Paper I for trailed exposures are therefore valid for the present observations, and may be considered conservative.

To estimate the limits for detection of multiple images in the coarse track–guided (untrailed) exposures, which constitute

TABLE 1

SUMMARY OF OBSERVATIONS

Quasar	Other Name[1]	Observation Date	Program Number	PC position[2] of Quasar	Offset[3]	Trail[4] Rate	V^5_{obs}	V^6_{tab}	Z	$-Mv^7$	Comments
0002 − 008	UM197	13/05/91	3158	6(209,292)	2.6	1.5	18.6	18	2.18	25.8	D
0002 + 0507	UM18	09/07/91	3158	6(125,201)	6.5	1.3	16.4	16.21	1.89	27.3	
0004 + 171		06/08/91	3158	6(550,595)	18.9	3.4	18.7	18.5	2.89	25.9	
0007 − 0004	UM208	16/09/91	3158	6(509,360)	11.4	0.4	18.5	17	2.31	26.9	
0007 − 4239		19/07/91	3158	missed	> 24	1.1					
0012 + 0040	UM222	18/09/91	3158	7(306,199)	17.4	1.0	18.4	17	1.46	26.0	
0013 − 0029	UM224	22/09/91	3158	6(61,254)	8.7	1.6	18.1	17	2.09	26.7	F
0018 − 422		17/07/91	3158	6(52,148)	10.3	5.1	18.4	18.6	2.86	25.7	
0019 + 0107	UM232	18/09/91	3158	6(75,228)	8.2	1.1	17.6	17	2.13	26.8	
0021 + 0535	UM30	09/07/91	3158	7(233,37)	10.4	1.7	19.6	18	2.05	25.7	C
0024 + 22		05/08/91	3158	8(174,590)	37.8	7.7	17.0	16.57	1.11	25.9	A
0027 − 1836	UM664	21/06/91	3158	missed	> 24	1.7					
0029 − 1209	UM665	21/06/91	3158	6(87,145)	9.1	2.4	18.1	18	2.65	26.2	
0041 − 261		14/09/91	3158	7(207,340)	23.5	1.2	17.2	17.3	2.50	26.8	D,F
0041 − 2707		14/09/91	3158	7(336,267)	20.5	1.1	18.0	17.4	2.78	26.9	
0044 + 0131	UM276	19/07/91	3158	6(360,191)	5.2	0.9	18.0	17	1.59	26.2	
0049 + 0045	UM287	19/07/91	3158	8(557,673)	49.9	2.3	18.4	17	2.27	26.9	D,F
0049 + 0124	UM288	19/07/91	3158	6(178,53)	9.7	0.8	17.3	17	2.31	26.9	
0055 − 4139		09/07/91	3158	8(522,296)	37.9	1.	18.7	18	2.64	26.2	
0101 − 4216		10/07/91	3158	7(355,164)	16.3	1.2	17.2	17.5	1.90	26.0	
0102 − 4238		13/07/91	3158	8(267,161)	25.6	1.4	18.3	18	2.33	25.9	F
0109 + 17		17/07/91	3158	7(184,211)	18.1	1.2	18.6	18	2.15	25.8	
0114 − 0856	UM670	28/06/91	3158	8(314,216)	28.0	1.0	17.9	17.4	3.16	27.1	
0116 − 0210	UM315	28/06/91	3158	6(719,301)	20.0	1.0	17.9	18	2.05	25.7	D
0117 − 1803	UM671	13/07/91	3158	6(249,281)	1.0	1.5	17.6	17.3	1.79	26.1	D
0119 − 04		28/06/91	3158	6(240,239)	1.4	1.0	17.2	16.88	1.95	26.7	
0123 − 0209	UM322	28/06/91	3158	6(631,311)	16.0	1.2	18.1	18	1.93	25.6	G
0132 + 20		06/08/91	3158	6(343,318)	4.2	5.2	17.8	17.5	1.78	25.9	D
0132 − 1947	UM672	10/07/91	3158	8(35,45)	14.8	0.9	18.8	18.7	3.13	25.8	D
0136 + 176		08/08/91	3158	6(389,352)	6.6	2.7	18.6	18.5	2.73	25.7	
0136 − 231		10/07/91	3158	6(121,278)	6.1	1.4	18.0	18	1.89	25.5	D
0148 − 516		17/07/91	3158	missed	70.0	0.5					A
0201 + 36*B*		07/08/91	3159	6(214,328)	3.5	0.	17.9	17.5	2.90	26.9	I
0225 − 014		28/06/91	3159	7(266,300)	21.6	1.9	18.6	18.15	2.03	25.5	
0248 + 43		08/08/91	3159	7(283,115)	13.7	2.7	17.7	15.5	1.31	27.3	A
0252 + 0136		28/06/91	3159	7(27,445)	29.7	1.9	17.8	18.06	2.45	26.0	H,F
0256 − 0000		28/06/91	3159	8(721,209)	43.5	2.3	17.8	18.72	3.36	25.9	D
0256 − 005		28/06/91	3159	8(362,61)	26.8	1.5	17.8	17.2	1.99	26.4	
0301 − 0035		28/06/91	3159	missed	> 24	2.7					
0302 − 0019		28/06/91	3159	6(186,453)	8.8	1.7	17.6	18.37	3.28	26.2	D
0347 − 241		11/08/91	3159	8(734,115)	42.6	1.3	17.4	17.5	1.88	26.0	
0355 − 48		23/04/91	3159	6(240,261)	1.0	g	16.7	16.38	1.01	25.9	
0438 − 166		20/04/91	3159	6(253,237)	1.2	g	18.1	17.65	1.96	25.9	
0438 − 43		19/04/91	3159	6(248,258)	0.7	g	19.1	18.8	2.85	25.5	
0451 − 28		19/04/91	3159	6(243,262)	0.9	g	18.3	18.5	2.56	25.6	
0451 − 418		11/08/91	3159	8(547,204)	36.7	1.3	18.0	18.2	2.13	25.6	I
0453 − 423		11/05/91	3159	8(158,208)	23	1.0	17.3	17.06	2.66	27.1	D
0528 − 250		19/04/91	3159	6(255,254)	0.5	g	17.9	17.24	2.76	26.9	
0731 + 65		20/04/91	3159	6(246,245)	1.1	g	18.4	18.5	3.03	25.9	
0747 + 611		20/04/91	3159	6(238,228)	1.8	g	17.3	17.5	2.49	26.6	A
0830 + 115		25/04/91	3159	6(236,260)	1.2	g	18.1	18.5	2.97	25.9	
0933 + 733		24/04/91	3159	6(502,360)	12	g	17.2	17	2.52	27.1	B
1017 + 1055		23/05/91	3156	missed	> 24	0.7					
10370 − 271		23/04/91	3156	6(255,260)	0.4	g	17.5	17.4	2.18	26.4	
1038 + 065	4C06.41	02/06/91	3156	6(243,264)	0.9	g	16.6	16.7	1.27	26.0	
10382 − 272		23/04/91	3156	6(243,263)	0.9	g	17.9	17.9	2.32	26.0	
1039 + 582		10/06/91	3156	7(235,253)	19.6	0.8	17.8	17.5	1.47	25.5	F
1045 + 60	4C60.15	23/05/91	3156	8(74,330)	25	1.0	17.9	17.5	1.72	25.8	
1116 + 603		10/06/91	3156	8(109,210)	22.3	1.0	17.7	16.5	2.63	27.7	

TABLE 1—*Continued*

Quasar	Other Name[1]	Observation Date	Program Number	PC position[2] of Quasar	Offset[3]	Trail[4] Rate	V^5_{obs}	V^6_{tab}	Z	$-Mv^7$	Comments
1117 + 535		02/06/91	3156	6(240,228)	1.8	g	17.6	18	1.92	25.6	
1133 + 1306		23/05/91	3156	7(217,593)	33	0.6	19.2	18.8	2.87	25.5	D
1136 + 1214		23/05/91	3156	missed	> 24	0.9					A
1137 + 30	US2778	23/05/91	3156	7(265,653)	36	0.7	16.8	16.9	1.57	26.3	
1138 + 584		20/05/91	3156	7(311,92)	12	1.9	17.7	18	2.40	26.0	
1139 + 2833	US2828	15/06/91	3156	missed	> 24	1.7					
1139.5 + 286	US2813	23/05/91	3156	6(92,122)	9.5	1.0	17.8	17.6	1.69	25.7	
1146 + 111*D*		23/05/91	3156	5(444,60)	19	1.0	17.6	17.6	2.12	26.2	F
1148 + 38		29/04/91	3156	6(232,251)	1.4	g	17.3	17.04	1.30	26.6	
1148 − 00		07/07/91	3156	7(183,412)	26.7	2.6	17.2	17.6	1.98	26.0	D
1155 − 1811	POX30	07/07/91	3156	8(339,245)	30.2	2.9	19.0	18	2.25	25.9	
1157 + 014		22/07/91	3156	6(56,253)	8.9	0.7	17.4	17.74	1.98	25.9	
1158 − 1842	POX42	27/07/91	3156	7(412,70)	13.4	0.9	17.2	17.01	2.44	27.0	
1159 + 123		19/04/91	3156	6(239,244)	1.3	g	17.6	17.5	3.51	27.2	
1202 − 20	POX62	23/04/91	3156	6(227,250)	1.6	g	18.8	18	2.17	25.8	
1206 + 1155		19/04/91	3156	6(257,228)	1.5	g	17.8	17.9	3.10	26.6	
1206 + 459		02/05/91	3156	6(237,228)	1.9	g	15.6	15.79	1.15	26.5	
1208 + 1011		22/07/91	3156	6(67,252)	8.4	0.9	17.9	17.5	3.80	27.4	A
1209.1 + 10.7		15/06/91	3156	missed	> 24	0.9					
1213 + 0922		11/06/91	3156	8(641,351)	43.4	1.0	18.4	17.2	2.71	27.0	D
1215 + 113		19/04/91	3156	6(245,250)	1.0	g	17.1	16.86	1.39	26.1	
1215 + 33		22/05/91	3156	7(180,77)	4	2.1	18.1	17.5	2.60	26.7	
1221 + 545		19/06/91	3156	6(225,316)	2.8	2.0	18.4	18	2.10	25.7	D
1228.0 + 07.8		10/06/91	3156	missed	> 24	1.5					
1228.5 + 07.6		11/06/91	3156	missed	> 24	0.9					
1228.7 + 07.7		13/06/91	3156	6(182,231)	3.7	1.4	18.0	17.6	2.39	26.4	
1241 + 176		23/05/91	3156	8(65,65)	15	1.2	16.1	16.3	1.27	26.4	F
1244.9 + 34.7		29/04/91	3156	6(244,261)	0.8	g	18.7	18	2.48	26.1	
1246 + 3746	BSO1	11/06/91	3156	5(652,231)	36.8	0.9	17.3	16.98	1.24	25.7	D
1247 + 268		27/07/91	3156	5(97,280)	12.9	0.2	15.7	15.9	2.04	27.8	
1248 + 401		20/06/91	3156	missed	> 24						
1256 − 17		10/06/91	3156	missed	> 24	1.0					
1257 + 34	B201	29/04/91	3156	6(237,254)	1.2	g	16.8	16.79	1.37	26.1	
1258 + 2839	W61972	07/07/91	3156	8(667,47)	38.9	3.	18.0	17.75	1.92	25.8	
1259 + 3427	BSO6	23/07/91	3156	8(283,78)	24.1	0.9	18.1	17.87	1.95	25.7	D
1303 + 3121	W21541	10/08/91	3156	8(172,573)	37.1	2.6	19.8	17.7	2.04	26.0	D
1304 − 1207	POX123	16/08/91	3156	6(425,253)	7.0	1.8	17.8	18	2.28	25.9	D
1305 + 3032	W22722	12/08/91	3156	6(242,209)	2.5	1.1	17.4	17.85	1.75	25.5	
1309 + 3402	BSO8	16/08/91	3156	missed	> 24						
1309 − 056		20/08/91	3156	8(435,130)	31.0	1.2	17.7	17.44	2.18	26.4	
1311 − 270		22/04/91	3156	6(247,254)	0.8	g	17.7	17.43	2.19	26.4	A
1315 + 4722		06/07/91	3156	7(119,186)	17.8	2.4	18.4	18	2.59	26.1	A
1315 + 605		06/07/91	3156	5(225,402)	19.4	2.2	18.9	18	1.98	25.6	A
1317 + 2743	TON153	15/08/91	3156	8(83,49)	16.4	1.8	15.9	15.98	1.02	26.3	D,H
1318 + 2903	TON155	23/06/91	3156	7(94,616)	36.0	0.9	17.4	17.27	1.70	26.0	
1327 − 206		21/07/91	3156	6(120,227)	6.3	1.1	16.9	17.04	1.16	25.5	A
1336 + 135		22/06/91	3156	6(476,711)	21.3	0.9	18.3	18.5	2.42	25.5	
1340 + 0959		22/08/91	3156	6(96,265)	7.2	1.5	18.8	18.5	2.94	25.9	
1347 + 1116		02/07/91	3156	6(260,269)	0.3	1.0	18.9	18.5	2.69	25.7	D
1352 + 011		14/07/91	3156	6(535,610)	19.0	3.7	16.3	16.04	1.12	26.4	F
1358 + 1134		07/07/91	3156	8(715,59)	41.1	2.5	17.8	16.5	2.57	27.6	
1400 + 0935		24/08/91	3156	7(219,55)	11.3	1.2	19.1	18.5	2.98	25.9	G
1402 + 044		18/08/91	3156	6(610,446)	16.9	1.5	19.1	18.5	3.20	26.0	D
1402 − 012		25/08/91	3156	8(679,345)	44.7	1.8	18.4	18.16	2.51	25.9	D
1409 + 0930		16/08/91	3156	6(528,538)	16.4	1.7	18.3	18.6	2.85	25.7	D
1410 + 0936		25/08/91	3156	6(397,114)	8.6	2.0	18.0	18.8	3.24	25.8	
1413 + 373		15/08/91	3156	missed	> 24	0.8					
1429 + 1153		15/08/91	3156	6(301,171)	4.3	2.2	18.3	18.6	3.01	25.8	G
1438 − 347		30/04/91	3156	6(246,254)	0.8	g	17.2	17	1.15	25.5	
1448 − 232		10/05/91	3156	7(377,138)	15	1.2	17.2	16.96	2.20	26.9	F
1451 + 1223		07/08/91	3156	6(41,253)	9.6	1.4	19.1	18.6	3.25	26.0	D
1455 + 1221		07/07/91	3156	5(106,375)	14.1	2.2	18.3	18.7	3.06	25.8	
1520 + 41	SP43	12/05/91	3156	5(158,62)	20	4.2	18.5	17.5	3.10	27.0	
1522 + 101		07/07/91	3156	8(446,120)	31.2	2.6	16.2	15.65	1.32	27.2	A
1548 + 0917		07/07/91	3156	8(112,109)	19.6	2.4	18.0	17.5	2.74	26.8	D

TABLE 1—*Continued*

Quasar	Other Name[1]	Observation Date	Program Number	PC position[2] of Quasar	Offset[3]	Trail[4] Rate	V^5_{obs}	V^6_{tab}	Z	$-Mv^7$	Comments
1634+176		03/08/91	3156	6(277,42)	9.5	0.6	18.7	18	1.89	25.5	
2021−330		19/06/91	3156	6(143,439)	9.2	2.9	16.4	16.3	1.47	26.7	A
2040−374		20/06/91	3156	6(698,519)	21.7	1.2	18.1	17.84	2.27	26.0	
2040−400		18/06/91	3157	6(198,422)	7.4	2.1	17.8	18.1	2.07	25.6	
2055−440		19/06/91	3157	7(399,84)	13.7	3.2	17.6	17.9	2.06	25.8	
2121+053		22/04/91	3157	6(260,240)	1.0	g	19.7	17.5	1.87	26.0	
2126−15		06/06/91	3157	6(247,263)	0.7	g	17.2	17.3	3.27	27.3	A
2131−42	HA2	18/05/91	3157	missed	59	1.4					E
2131−46	HA5	18/05/91	3157	7(333,623)	35	0.4	18.5	18.47	2.94	25.9	
2134+004		30/04/91	3157	6(267,243)	0.9	g	17.3	16.79	1.93	26.8	
2136+141		24/04/91	3157	7(114,250)	20	3.1	18.6	18.5	2.42	25.5	
2149−306		16/05/91	3157	8(316,318)	30	2.5	17.8	18.4	2.34	25.9	
2150+05		10/05/91	3157	6(320,77)	8.3	2.5	18.0	17.77	1.97	25.8	
2153−204		14/05/91	3157	6(122,170)	7.2	1.9	17.5	17.01	1.30	25.8	
2156+29		22/04/91	3157	6(256,264)	0.3	g	19.4	17.5	1.75	25.9	
2158−214		14/05/91	3157	6(176,596)	14.8	1.8	17.9	18.15	2.07	25.6	
2204−408		18/05/91	3157	8(689,200)	41	0.5	17.9	17.57	3.17	27.0	F
2204−573		16/07/91	3157	8(97,265)	23.9	0.6	17.5	17.36	2.72	26.9	
2212−299		22/09/91	3157	7(383,349)	24.3	1.4	17.3	17.44	2.70	26.8	
2219−394		06/09/91	3157	6(137,376)	7.3	2.0	17.8	17.74	2.02	25.9	D
2222−396		22/09/91	3157	7(539,347)	26.5	1.6	17.8	17.9	2.18	25.9	
2223+21		06/06/91	3157	6(249,235)	1.4	g	17.7	18	1.95	25.6	
2227−3928		16/09/91	3157	6(94,126)	9.3	1.1	18.6	18.8	3.45	25.9	
2228−399		04/09/91	3157	5(399,339)	26.1	0.4	18.3	18.3	2.20	25.5	
2236−2416	UM656	18/09/91	3157	7(50,529)	32.8	1.4	17.8	18.1	2.45	25.9	
2240−419		19/05/91	3157	7(607,207)	17	2.4	17.8	18	2.08	25.7	
2246−389		02/09/91	3157	7(182,536)	32.0	2.7	17.8	17.9	2.12	25.9	F
2254+024		20/07/91	3157	8(436,187)	32.2	0.5	18.2	17	2.09	26.7	F
2258−391		06/09/91	3157	7(61,154)	17.6	1.2	17.9	18	2.05	25.7	
2300−352		02/09/91	3157	6(66,145)	9.9	2.5	18.4	17.9	2.84	26.4	
2302+029		06/09/91	3157	6(219,231)	2.3	1.9	15.9	16.1	1.04	26.2	
2335−18		14/09/91	3157	7(57,628)	36.8	1.2	17.2	17.34	1.44	25.6	D
2341+010	UM175	13/05/91	3157	7(480,37)	14	1.2	18.5	18.6	1.96	25.6	C
2341−2333	UM660	19/09/91	3157	6(479,461)	12.6	1.5	17.8	18.1	2.82	26.2	F
2345+061		30/05/91	3157	6(251,256)	0.6	g	18.2	17.5	1.54	25.6	
2348−011	UM184	13/05/91	3157	6(81,600)	16.5	1.3	18.3	18	3.01	26.4	D
2348−4025		30/05/91	3157	6(269,134)	1.0	g	18.0	18.6	3.31	26.0	
2351−154		30/05/91	3157	6(257,242)	0.9	g	18.7	17	2.66	27.2	
2352−455		30/05/91	3157	6(246,251)	0.9	g	19.2	17.5	1.86	26.0	
2355−389		29/05/91	3157	6(274,203)	2.6	g	18.1	18.4	2.85	25.9	
2357−326		30/05/91	3158	6(256,232)	1.4	g	18.6	17	1.27	25.7	F
2357−348		29/05/91	3157	6(255,232)	1.4	g	17.6	17	2.07	25.9	
2358−161		30/05/91	3158	6(235,263)	1.2	g	18.4	18	2.04	25.7	
2359+0653		13/07/91	3158	6(526,68)	14.1	1.5	18.4	18.8	3.24	25.8	D
2359−0216	UM196	18/09/91	3158	7(304,188)	16.9	0.9	18.7	18	2.82	26.3	F

[1] Listed for objects for which Véron-Cetty & Véron 1987 give a name that does not include the coordinates.
[2] Planetary Camera (PC) CCD number (5–8) and pixel coordinate with the origin at the PC apex.
[3] From the designated position on PC-6 (263, 263), in arcseconds.
[4] In milliarcseconds s^{-1}; "g" designates a coarse track–guided exposure.
[5] V-magnitude determined from this *HST* exposure, accurate to $\approx \pm 0.2$ mag.
[6] V-magnitude tabulated by Véron-Cetty & Véron 1987.
[7] Assuming $H_0 = 100\ \mathrm{km\ s^{-1}\ Mpc^{-1}}$, $q_0 = 0.5$.

COMMENTS.—(A) See "Notes on Individual Objects." (B) Guided exposure, but quasar offset by 12″ for unknown reasons. (C) Quasar image split between PC-6 and PC-7. (D) Quasar not verified to be in the field of view, but likely present based on brightness and/or expected absence of additional objects. (E) Quasar just off PC-8. (F) Possibly some point-spread function asymmetry at 0.″1–0.″2 scales. (G) Identification uncertain. (H) Quasar image split between PC-7 and PC-8. (I) Attempted observation also in Paper I.

about one-fourth of the exposures, we have carried out additional simulations. The point-spread function of a bright quasar (1206+459) from one of the guided exposures was scaled down to have the total number of counts of a $V = 18.7$ object (the magnitude being chosen for consistency with the trailed image detection limits above). A secondary image, a scaled version of the point-spread function, was then added with a grid of separations and magnitude differences from the primary image. Simulated readout noise, Poisson noise, and cosmic-ray events were added to the simulated image. For each separation, the maximum magnitude difference for which the secondary image was discernible was noted. To check the

TABLE 2

DETECTION LIMITS FOR GUIDED IMAGES

Separation (arcsec)	Maximum Detectable Magnitude Difference
0.12	0.5
0.16	1.5
0.2	2.0
0.3	2.5
0.4	3.0
0.5	3.0
0.6	3.0
0.8	3.5
1.0	3.5
1.5	3.5
2.0	3.5

objectivity of this procedure, we repeated it in a blind fashion: One of us (D. M.) created the simulated images, and another (B. Y.) searched them for the secondary components. The results from the blind test were almost identical to those of the first test. The results of these simulations are summarized in Table 2.

The detection limits in Table 2 for the guided images are similar to those found in Paper I for the trailed exposures. At separations of 0".4 and larger, the guided exposures can detect secondary images 0.5 mag fainter than the trailed exposures. The limits are similar for the two types of exposures because of two effects working in opposite directions: The secondary image has a larger contrast above the background in the guided images, but a trailed secondary image is easier to recognize and distinguish from a cosmic-ray event (the trail direction and length are the same as in the bright primary image).

3.2. *Notes on Individual Objects*

0024+22.—The trail rate for this quasar is unusually large, 7.7 mas s^{-1}. The long trail and the brightness of the object ($V = 17.0$) combine to stretch and make visible some of the faint features in the PSF, creating false "secondary images" at separations of 0".1–0".7 from the primary image. There is a real 20th magnitude point source 6".3 to the northeast, at position angle (P.A.) 21°.6. Broad-band CCD exposures were taken at the Palomar 1.5 m telescope on 1990 November 21 through Schombert *B* and Thuan-Gunn *g* and *i* filters in 3" seeing. These exposures show that the quasar and the point source 6".3 to its northeast have, within the errors, similar colors. This object therefore merits further study.

0148−516.—It was unclear whether the sole object in the PC field of view, a 14.9 mag point source on PC-8, was the targeted quasar, which has a tabulated magnitude of 18.2. To investigate the possibility that the quasar has undergone a large outburst in brightness, *B*, *V*, *R*, and *I* CCD images were kindly obtained by S. Raychaudhury and G. Williger on 1991 October 30 at the CTIO 0.9 m telescope. The images show that the quasar is at its usual brightness and that the object imaged by *HST* is probably a star 50" northwest of the quasar, in which case the *HST* pointing is off by 70". The ground-based image also shows a 19.5 mag star 37" northeast of the quasar which, at the PC orientation, should have appeared on PC-6 had the object in PC-8 been the quasar.

0248+43.—The field around this quasar has a relatively large number of objects, mostly faint galaxies, and has been studied by Sargent & Steidel (1990), Womble at al. (1990), Kollatschny et al. (1991), and Borgeest et al. (1991). The *HST* image shows a disturbed galaxy 14" east of the quasar, a faint galaxy 10".7 northeast of the quasar, and a $V = 19$ point source 5".9 south of the quasar. The quasar is 2 mag fainter than tabulated by Véron-Cetty & Véron (1987). Womble et al. (1990) and Sargent & Steidel (1990) showed that the disrupted galaxy had a double nucleus and an extended nebulosity emerging west in front of the quasar. They concluded that the galaxy is in the final stages of a merger. The *HST* image, a section of which is shown in Figure 1 (Plate 1) resolves well the inner region of the galaxy and shows that the two nuclei have curved extensions pointing toward each other, supporting the merger picture. The brighter of the two nuclei has an unresolved core, supporting the spectroscopic evidence by Kollatschny et al. (1991) that nuclear activity is taking place. Womble et al. (1990) also obtained spectra for several of the objects in the field, and found that the merging galaxy is at redshift 0.052, the faint galaxy to the northeast is at redshift 0.24, and the point source to the south of the quasar is probably a Galactic star.

0747+611.—Crampton et al. (1989) noted that there was an additional object east of this quasar. This 19.5 mag point source is easily discernible in the *HST* exposure, at a separation of 1".7 and P.A. 89°.3. Spectroscopy of the quasar and the fainter point source carried out at the Palomar 5 m telescope on 1991 September 5 shows that the fainter object has the spectrum of a foreground Galactic star.

1136+1214.—The 19.5 mag object on PC-5 appears to be resolved into a brighter image and two secondary images, about 2 mag fainter, to its south at separations of 0".1 and 0".2. The quasar, however, is expected to have $V = 17.6$ rather than 19.5, and the only other object in the PC field of view is a faint point source 11".4 to the east which is not visible on the Palomar Sky Survey. In an attempt to identify the field, we obtained a 35 minute exposure through the *V*-filter with the ARC 1.8 m telescope on 1991 June 3. The resulting image shows no objects that are 11" from the quasar. On the other hand, two neighboring stars do have faint companions at that separation. We conclude that the targeted quasar was missed.

1208+1011.—*HST* and VLA observations of this object were described in detail in Maoz et al. (1992). In the Snapshot exposure the quasar is resolved into two or possibly three components: a central bright component ($V = 18.3$), a $V = 19.8$ component at P.A. 160° and separation 0".5, and possibly a $V = 20.0$ component 0".1 from the bright component, at P.A. 40°. A repeated coarse track–guided observation carried out on 1991 December 23 confirms the brightness ratio and separation between the quasar and the component 0".5 from it, but fails to show the close 0".1 component, indicating that the latter was probably an artifact of the trailed point-spread function. This recent observation will be described in detail in a separate paper. The VLA exposure showed that this quasar is radio-quiet, with a 3 σ upper limit of 0.6 mJy on the radio flux at a wavelength of 6 cm. Further *HST* photometry and spectroscopy will determine whether this is a gravitationally lensed system. It is the most promising lens candidate in the currently observed sample.

1311−270.—This guided exposure reveals a faint object ($V \approx 22.5$) 3".9 north of the quasar at P.A. 340°.3. S. Djorgovski (private communication) has found, based on *B*, *V*, *R* images from CTIO, that the companion is much redder than the quasar and is therefore almost certainly a foreground star.

1315+4722.—There is a faint diffuse object, likely a distant

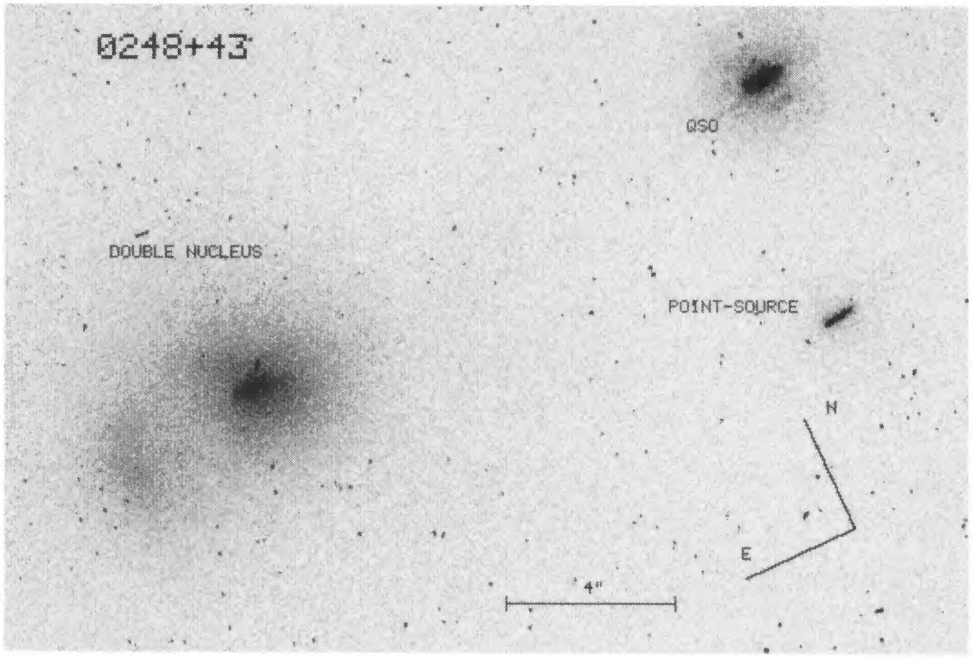

FIG. 1.—Section of the PC image of the quasar 0248+4302 and the double-nucleus galaxy to its east. The *HST* image shows clearly that each of the two nuclei in the galaxy have tidal tails pointing toward each other, supporting the interpretation that a merger is in process. The point source south of the quasar is probably a Galactic star.

MAOZ et al. (see 394, 56)

galaxy, 5″ west of the quasar. The galaxy is visible in the Palomar Sky Survey.

1315+605.—The quasar is 10″ south of a faint galaxy and 5.″6 east of a point source that is 1 mag brighter than the quasar, probably a Galactic star.

1327−206.—In the Palomar Sky Survey plates, this quasar appears to be behind the tidal arm of a large (~a few arcminutes) disrupted galaxy. The diffuse tidal arm is too faint to be seen in the *HST* exposure, and the quasar image appears normal for a point source.

1522+101.—There are two faint galaxies, 5″ and 9.″2 north of the quasar at P.A. 30° and P.A. 27°, respectively.

2021−330.—In the finding chart published by Peterson & Bolton (1973), it is hard to distinguish the quasar from a bright stellar object 11.″4 east of it. The published photometric measurements for this quasar vary from $V = 16.3$ to $V \geq 17.5$, and we suspect that confusion about the identity of the quasar may be responsible for the range in brightnesses. The 19.5 mag quasar has a 21 mag companion 1.″8 east of it, at P.A. 114°. Spectroscopy by Véron et al. (1990) shows the companion is an early-type star.

2126−15.—The *HST* exposure shows a faint diffuse object 6″ west of the quasar.

3.3. *Notes on Some Objects from Paper I*

0051+29.—The identification of this quasar was uncertain in the *HST* exposure described in Paper I, since the only other object appearing in the field of view was too faint to be seen in our finding charts. We obtained a 600 s *g*-band exposure at the Palomar 1.5 m telescope on 1991 October 12. The ground-based image shows the 21 mag object 37″ southeast of the quasar, confirming that the quasar was indeed in the field of view in the Paper I *HST* image.

0308+1902.—The Paper I *HST* exposure shows three faint objects southeast, south, and west of the quasar, none of which appear on our finding charts. A 600 s *g*-band exposure taken on 1991 October 12 with the Palomar 1.5 m telescope shows the southern and western objects at the required separations from the quasar of 53″ and 10″, respectively. (The southeast object was not in the field of view of the ground-based image.) The quasar was therefore in the field of view in the Paper I *HST* image.

0348+06.—The PC image in Paper I showed, apart from the quasar, a single faint object, making the quasar's identification uncertain. A 600 s *g*-band exposure with the Palomar 1.5 m telescope on 1991 October 12 shows a 21.5 mag object at the required separation 16.″5 west of the quasar, confirming that the quasar was observed in the Paper I *HST* image.

0454+039.—Two faint objects in the Paper I *HST* exposure, 15″ southwest and 20″ southeast of the quasar, are detected in a 1500 s *g*-band exposure we obtained on 1991 October 12 with the Palomar 1.5 m telescope. This confirms that the quasar was in the field of view in the *HST* exposure.

4. ENGINEERING RESULTS

The mode of operation of the Snapshot Survey makes it a useful tool for obtaining engineering data on the *HST* systems. As reported in Paper I, the Snapshot monitoring of the pointing error and the gyroscope drift rate revealed that stellar aberration corrections were not being applied when the telescope was under gyro control. The correction of this problem in 1991 April immediately improved the pointing and guiding performance of the telescope. From Table 1 we find that the mean drift rate during the period reported here was 1.6 ± 1.0 mas s^{-1}, where the error is the root mean square. This compares with the value 4.4 ± 1.4 mas s^{-1} of Paper I. Similarly, the mean pointing error is 20″ ± 13″. In Paper I, the pointing error was estimated to be 20″–30″ but could not be accurately determined because in about half of the exposures the quasar was altogether outside the field of view, which was often unidentified or empty. In the current observations only 15 exposures, i.e., 11% of all the gyroscope-guided exposures, missed the target. We have found no correlation between the pointing error and the drift rate, or between each of them and time of observation, right ascension, or declination of the targets.

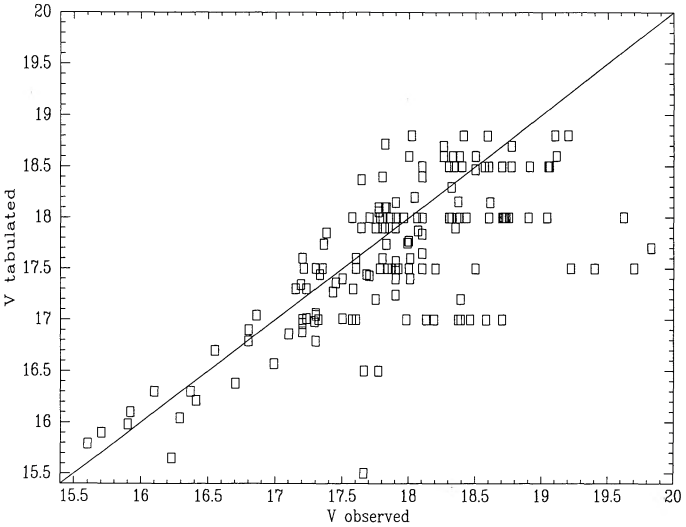

FIG. 2.—*V*-band magnitudes, as tabulated by Véron-Cetty & Véron (1987), of the quasars observed in this paper versus the magnitudes measured from the *HST* exposures. The diagonal line is $V_{tab} = V_{obs}$. Excluding some of the deviant points that have integer or half-integer tabulated magnitudes (inaccurate ground-based photometry) and several outliers (probably the result of variability), the observed magnitudes follow the diagonal line well, indicating that the PC sensitivity and linearity are in accord with prelaunch expectations.

The data in Table 1 also allow us, to some extent, to study the performance of the PC. Individually, the quasars in the sample are poor flux standards because many of them have poorly measured magnitudes and because probably all quasars vary in brightness, given enough time. Nevertheless, one can compare statistically the expected versus observed magnitudes of the sample in order to search for overall changes or trends in the instrument sensitivity.

Figure 2 is a plot of V_{tab} versus V_{obs} from Table 1, i.e., the quasar magnitudes tabulated by Véron & Véron-Cetty (1987) versus the magnitudes determined from the *HST* exposures using the preflight PC sensitivity predictions (Griffiths 1990). The diagonal line, shown for reference, has a slope of 1. It is remarkable that most of the points lie along the diagonal line. Most of the excess of objects that lie far below the line (i.e., are 1–2 mag fainter than expected) have cataloged magnitudes with integer or half-integer values; such magnitudes are usually rough estimates based on photographic plates and are expected to be inaccurate. The remaining points show a trend of larger scatter about the expected magnitude with increasing magnitude, but no systematic change in sensitivity. Some of the larger scatter at faint magnitudes is probably due to the decreasing accuracy of the ground-based measurements, while

some of the scatter at all magnitudes and the outlying points are surely due to intrinsic variability. Accounting for these factors, we estimate the absolute photometric accuracy of the PC in the F555W filter to be about ± 0.2 mag. This is consistent with an earlier estimate by Holtzman et al. (1991).

5. THE FREQUENCY OF GRAVITATIONAL LENSING

In this section we compare the lensing frequency observed in our sample with that expected under various cosmological models and assumptions. In what follows, we will assume that our sample has uncovered one new gravitationally lensed quasar, the $z = 3.8$ quasar $1208+1011$. Our conclusions could change significantly if it eventually turns out that $1208+1011$ is not lensed or, on the other hand, that some of the quasars with point sources within several arcseconds, noted in § 3, are lensed.

Of the 168 quasars scheduled in the observations described here, 153 were successfully observed (i.e., the quasar was in the PC field of view). One of the targets ($0451-418$) was assumed to have been imaged also in Paper I. The present observations therefore supplement the observed sample discussed in Paper I by 152. Together with the 32 quasars observed in Paper I (including the four quasars confirmed in § 3.3), the current total observed sample constitutes 184 quasars. In computing the observed number of lenses, one must account for previously known lenses which passed the sample criteria but were eliminated from the sample to avoid duplication of other *HST* imaging programs (see Paper I). There were four such lensed quasars in our originally selected sample ($0142-100$, $0957+561$, $1115+080$, and $1413+117$). Had they been included, we would have detected them as lens candidates. It is debatable whether $0957+561$ should be included among these four quasars, because it is lensed by the combined influence of a galaxy and a cluster of galaxies, an effect that we do not take into account when calculating the predicted lensing frequency below. On the other hand, it can be argued that this quasar would have been lensed by the lensing galaxy alone and detected as such by the Snapshot Survey even in the absence of the lensing cluster. This ambiguity has a minor effect on the derived lensing frequency of the survey. We choose to include $0957+561$ among the four known lensed quasars. Since we have observed just over one-half of the total sample of 354 quasars, we will assume that we would have rediscovered two of the four known lenses. Together with $1208+1011$, the detection rate is then 3/184. (Twenty-seven quasars which were not previously known to be lensed and which passed the sample criteria were also eliminated from the sample to avoid duplication with other *HST* programs. Since we do not know whether these quasars are lensed or not, they need not be accounted for.)

The predicted number of multiply imaged lensed quasars in the observed sample is found by computing for each quasar its probability of being lensed and summing the probabilities over the whole sample. The probability that a quasar is lensed is the product of its optical depth τ to lensing by an intervening galaxy, and its magnification bias B. B is the factor by which lensed quasars are overrepresented among quasars of a given magnitude because fainter quasars have been amplified to that magnitude by lensing (Turner, Ostriker, & Gott 1984; Kochanek 1991b; Fukugita & Turner 1991; Paper I). We make no correction for lensed quasars that are missed as a result of our detection limits, i.e., because their largest component separations are smaller than we can detect and/or the component magnitude differences are larger than we can detect. We estimate that this fraction of undetected lensed quasars is of order 10%.

For the optical depth τ under various cosmologies, we will use the formulae presented in Paper I. For flat ($k = 0$) cosmologies with arbitrary values of the fraction of the closure density Ω_0, we use (Turner 1990)

$$\tau(z) = 0.5\left(\frac{F}{30}\right)\left(\int_1^{z+1} \frac{dw}{(\Omega_0 w^2 - \Omega_0 + 1)^{1/2}}\right)^3 , \qquad (1)$$

where, as in Paper I, we take $F = 0.045$ for the dimensionless parameter proportional to the lensing effectiveness of a population of galaxies represented by singular isothermal spheres. The integral in equation (1) is evaluated numerically. As in Paper I, we have multiplied the optical depth by a factor of 0.5 to account for the finite core size of galaxies (Fukugita & Turner 1991).

For the magnification bias B we will use the expressions derived in Paper 1 from the quasar luminosity function of Boyle et al. (1987):

$$B(M_B, z) = \begin{cases} 17.79 \times 10^{0.24(M^* - M_B)} - 20.14 , & M_B \le M^* - 0.75 , \\ 1.28 \times 10^{0.96(M^* - M_B)} , & M^* - 0.75 \le M_B \le M^* , \\ 1.28 , & M_B \ge M^* , \end{cases} \qquad (2)$$

where M_B is the absolute magnitude of the quasar in the B band. $M^*(z)$ is the absolute magnitude of the break in the luminosity function and is given by

$$M^*(z) = -2.5k_L \log (1 + z) + M_0^* , \qquad (3)$$

where $k_L = 3.5$ and $M_0^* = -21.75$ for $H_0 = 50$ km s^{-1} Mpc^{-1} and $q_0 = 0.5$. Most of the quasars do not have measured B-magnitudes. We assume a typical $B-V = 0.2$ in the quasar rest frame. To obtain M_B, we therefore add 0.2 mag to the values of M_V in Table 1, and subtract 1.5 mag to transform from $H_0 = 100$ to the value of $H_0 = 50$ assumed by Boyle et al. (1987). Note that, although $B(M_B, z)$ was calculated in Paper I for a certain choice of cosmology, it depends only on the slopes of the luminosity function, and on the difference $(M^* - M_B)$. Since all of these are independent of cosmology, so is B.

Table 3 presents the results of the calculations of the predicted lensing frequency. The columns of the table give, for six different combinations of cosmological parameters, the expected number of lensed quasars and (in parentheses) the probability of seeing the actually observed number of lensed quasars (last column in Table 3) given the model and assuming Poisson statistics. The parameter $\lambda \equiv \Lambda/(3H_0^2)$ is the dimensionless form of the cosmological constant.

In the first row of entries in Table 3, all of the observed sample was included in the calculations, and the magnitudes of the quasars, necessary for computing the magnification bias, were taken from Véron-Cetty & Véron (1987) ($V_{\rm tab}$ in Table 1). As already pointed out, quasars vary, and this complicates the determination of the magnification bias. One may argue that it is the brightness of the quasar in the catalog that constitutes its "normal" brightness, so that $V_{\rm tab}$ is indeed the number to use. On the other hand, we have seen in § 4 that many of the cataloged magnitudes are simply inaccurate, which justifies

TABLE 3

PREDICTED AND OBSERVED NUMBERS OF LENSED QUASARS AND MODEL PROBABILITIES

METHOD OF CALCULATION	$\lambda = 0$		$\lambda + \Omega_0 = 1$				OBSERVED
	$\Omega_0 = 0$	$\Omega_0 = 1$	$\Omega_0 = 0$	$\Omega_0 = 0.1$	$\Omega_0 = 0.15$	$\Omega_0 = 0.2$	
Bias computed with V_{tab} (184 quasars)	3.1 (63%)	1.6 (22%)	24.3 (7×10^{-8})	9.7 (1%)	7.7 (5%)	6.4 (12%)	3
Bias computed with V_{obs} (184 quasars)	2.3 (40%)	1.2 (12%)	18.5 (1×10^{-5})	7.3 (6%)	5.8 (17%)	4.8 (30%)	3
Only $z < 2.5$ (125 quasars); bias computed with V_{obs}	1.7 (49%)	1.0 (73%)	11.0 (2×10^{-4})	5.2 (3%)	4.2 (8%)	3.5 (14%)	1

using the *HST* measured magnitudes for the bias computation. The second row in Table 3 gives the predicted number of lenses when the observed magnitudes (V_{obs} in Table 1) are used. Since, as seen in Figure 2, more quasars are fainter than cataloged rather than brighter, the magnification bias is lower and the predicted numbers are somewhat smaller.

The luminosity function used to derive equation (2) was observed by Boyle et al. (1987) for quasars at $z < 2.2$. The form of the luminosity function at higher redshifts is uncertain at present. In calculating the first two rows in Table 3, we assumed that the functional form found at $z < 2.2$ can be extrapolated to the higher redshifts of some of the quasars in our sample. To investigate the effect of this assumption on the results, in the third row of Table 3 we calculate the predicted number of lenses in our sample including only quasars with $z < 2.5$. Note that the observed number of lensed quasars is now only one, since two of the four previously known lenses removed from the original sample have $z > 2.5$ (0142−100 and 1413+117; having observed one-half of the entire sample, we assume we would have detected one of the remaining two), while the one new lens that we assumed to have found, 1208+1011, has $z = 3.8$. The magnification bias is calculated using V_{obs}. We see that the redshift constraint only strengthens the conclusion that the observed number of lenses is significantly lower than predicted by λ-dominated cosmologies, and is consistent with the predictions of $\lambda = 0$ models.

Among the various parameters, these calculations are most sensitive to the value assumed for the absolute magnitude of the break in the Boyle et al. (1987) quasar luminosity function, M_0^*. Varying this parameter within the 1 σ range quoted by them (± 0.5 mag) affects the magnification bias enough to lower or raise the predictions in Table 3 by factors of 1.6–1.8, depending on the combination of the other parameters in the table. However, this is an overestimate of the effect of the uncertainty in M_0^*, since M_0^* and the slopes of the luminosity function are not independent; for example, a brighter break magnitude, which would decrease the magnification bias and the prediction in Table 3, would also imply a steeper luminosity function slope at magnitudes brighter than M^*, which could compensate for the decrease.

The results in Table 3 argue against the domination of the universe by a cosmological constant (see, e.g., Carroll, Press, & Turner 1992 for a review). This supports the similar conclusions of Fukugita & Turner (1991) and Paper I. Kochanek (1992) also found that the redshifts of the lensing galaxies among known lensed quasars argue against flat cosmologies with $\lambda > 0.9$. The possibility of a nonzero λ has been recently raised again, mainly because of the "age problem"; i.e., if H_0 is larger than 80 km s^{-1} Mpc^{-1}, then the age of the universe is in conflict with the age of globular clusters, unless $\lambda > 0$. Moreover, if Ω_0 turns out to be less than unity, then a way to save the inflation model, which implies zero curvature, is to have nonzero λ, such that $\Omega_0 + \lambda = 1$. Among the various observational tests for $\lambda > 0$, the one using the frequency of quasar lensing is relatively direct and robust.

On the other hand, there are still enough uncertainties in the results presented here so that the cosmological constant scenario can be saved. Some of the possibilities are the following: (1) The luminosity function of quasars may be flatter than found by Boyle et al. (1987) or, as already noted, may have a break at brighter magnitudes, lowering the magnification bias. (2) F is overestimated owing to, for example, a more important role played by the finite-sized (rather than singular) cores of galaxies (e.g., Kochanek 1991b). (3) Evolution of the galaxy population, so that there are fewer galaxies at moderate and high redshifts (Mao 1991), or evolution of galaxy properties (e.g., larger galaxy cores at high redshifts). (4) Selection effects that remove lensed quasars from our sample; e.g., if lensed quasars are reddened by the lensing galaxy, then they will not be discovered by surveys selecting on the basis of blue color excess (Kochanek 1991b). (5) More realistic elliptical galaxy potentials may give a somewhat different lensing frequency prediction than the singular isothermal sphere galaxy model used here. A Monte Carlo simulation including the survey's selection criteria and detection limits (Kochanek 1991b) can investigate this possibility. It may also be argued that the predictions of the $\Omega_0 = 0.2$, $\lambda = 0.8$ model in Table 3 need to be scaled down by only a factor of 2 to coincide with our observations; Efstathiou, Sutherland, & Maddox (1990) find that such a value of Ω_0 is enough to reconcile the cold dark matter galaxy formation model with the excess power observed on large scales (see, however, Park 1991).

Once the parameters needed to make the theoretical lensing frequency prediction are better known, our observational result may constrain the models even more strongly. We also expect the observed sample of Snapshot quasars to double within the next year, thus improving the statistics.

6. CONCLUSIONS

We have presented results from the ongoing *HST* Snapshot Survey. Of the 184 quasars observed to date (constituting about one-half of the entire sample), one object, 1208+1011, shows subarcsecond structure and is a promising lens candidate.

The predicted lensing frequency of the sample has large uncertainties due to its dependence on a number of observational parameters. However, using the best-known values for

these parameters and assuming that among the quasars observed by the Snapshot Survey only 1208+1011 is lensed, the observed lensing frequency agrees well with the predictions of cosmologies with zero cosmological constant λ. The lensing frequency is considerably lower than predicted by λ-dominated cosmologies. However, such models can still be made to agree with the observations by allowing some of the parameters, e.g., the break in the quasar luminosity function, to take on extreme values. In any event, our present results establish that small image-separation quasar lensing is a rare phenomenon, affecting a fraction of a percent of our quasar sample. This is in conflict with the claims by several ground-based surveys for a high incidence of lensing among similar quasar samples.

The software corrections for stellar aberration when *HST* is under gyro control, implemented following the results of Paper I, have resulted in much lower measured trail rates and pointing errors in the present program than in the pilot program reported in Paper I. We will continue monitoring these and other engineering aspects of the *HST* performance throughout cycle 1 of operations.

We thank R. Giacconi and H. S. Stockman for their continued support of the Snapshot Survey as an STScI Director's Discretion program. We are grateful to P. Guhathakurta, S. Raychaudhury, and G. Williger for obtaining CCD images at CTIO; to S. Djorgovski for making available to us the results from some of his ground-based observations of lens candidates; to J. Gunn and M. Schmidt for obtaining a spectrum at the Palomar 5 m telescope; to W. Sargent and S. Strauss for obtaining CCD images at the Palomar 1.5 m telescope; to A. Gould, C. Kochanek, M. Strauss, and E. Turner for helpful discussions; and to M. Best for making the tables.

This work was supported by NASA grant NAG5-1618 (J. N. B., N. A. B., and D. P. S.), Space Telescope Science Institute grant GO-2775 (D. M.), and Hubble Fellowship HF-1013.01-90A (B. Y.).

REFERENCES

Bahcall, J. N., Maoz, D., Doxsey, R., Schneider, D. P., Bahcall, N. A., Lahav, O., & Yanny, B. 1992, ApJ, 387, 56 (Paper I)
Blandford, R. D., & Narayan, R. 1992, ARA&A, in press
Borgeest, U., Dietrich, M., Hopp, U., Kollatschny, W., & Schramm, K. J. 1991, A&A, 243, 93
Boyle, B. J., Fong, R., Shanks, T., & Peterson, B. A. 1987, MNRAS, 227, 717
Carroll, S. M., Press, W. H., & Turner, E. L. 1992, ARA&A, in press
Chang, K., & Refsdal, S. 1979, Nature, 282, 561
Crampton, D., McClure, R. D., Fletcher, J. M., & Hutchings, J. B. 1989, AJ, 98, 1188
Dar, A. 1992, Nature, in press
de Vaucouleurs, G., de Vaucouleurs, A., & Corwin, H. G. 1976, Second Reference Catalogue of Bright Galaxies (Austin: Univ. Texas Press)
Efstathiou, G., Sutherland, W. J., & Maddox, S. J. 1990, Nature, 348, 705
Fukugita, M., & Turner, E. L. 1991, MNRAS, 253, 99
Griffiths, R. 1990, WF/PC Instrument Handbook (Baltimore: Space Telescope Science Institute)
Gunn, J. E., et al. 1987, Opt. Engineering, 26, 779
Holtzman, J. A., et al. 1991, ApJ, 369, L35
Horne, K., & Ritchie, C. 1991, WFPC Instrument Report WFPC-91-01 (Baltimore: Space Telescope Science Institute)
Kochanek, C. S. 1991a, ApJ, 373, 354
———. 1991b, ApJ, 379, 517
———. 1992, ApJ, 384, 1
Kollatschny, W., Dietrich, M., Borgeest, U., & Schramm, K. J. 1991, A&A, 249, 57
Mao, S. 1991, ApJ, 380, 9
Maoz, D., et al. 1992, ApJ, 386, L1
Paczyński, B. 1986, ApJ, 304, 1
Park, C. 1991, ApJ, 382, L59
Peterson, B. A., & Bolton, J. G. 1973, Ap. Lett., 13, 187
Rauch, K. P., & Blandford, R. D. 1991, ApJ, 381, L39
Sargent, W. L. W., & Steidel, C. C. 1990, ApJ, 359, L37
Turner, E. L. 1990, ApJ, 365, L43
Turner, E. L., Ostriker, J. P., & Gott, J. R. 1984, ApJ, 284, 1
Tyson, J. A., Valdes, F., & Wenk, R. A. 1990, ApJ, 349, L1
Véron, P., Véron-Cetty, M. P., Djorgovski, S., Magain, P., Meylan, G., & Surdej, J. 1990, A&AS, 86, 543
Véron-Cetty, M. P., & Véron, P. 1987, A Catalogue of Quasars and Active Nuclei (3d ed.; Munich: ESO)
Womble, D. S., Junkkarinen, V. T., Cohen, R. D., & Burbidge, E. M. 1990, AJ, 100, 1785